An Approximate Link Equation for the Direct-Detected Optical PPM Link

Bruce Moision* and Hua Xie†

ABSTRACT. — We derive a simple, approximate link equation for a direct-detected, pulse-position-modulated (PPM) optical link. To enable this, we utilize a fixed field-of-view parameter. Scaling laws are determined from the link equation, and we show that the link may be divided into three regions as a function of the link parameters: a signal-power-dominant regime, a background-noise-dominant regime, and a bandwidth-limited regime. As a function of the range R, with all other parameters held constant, the data rate goes as $1/R^2$ in the signal-dominant regime, as $1/R^4$ in the noise-dominant regime, and saturates in the bandwidth-limited regime. An approximation to the optimum modulation order is determined for the signal-dominant case. The accuracy of the link equation is demonstrated by comparing its predictions with those produced by a link budget tool developed at JPL, showing good agreement. Finally, the equation is used to derive a critical data rate and noise power at which the link transitions from signal dominant to noise dominant.

I. Introduction

A link equation relates the conditions under which a communication link may be used to reliably transmit information. In this article, we develop a simplified link equation for an optical communications link, demonstrate its accuracy, and utilize it to predict a critical data rate above which background light is negligible. One can show that, over a range of target data rates and background noise levels, the most power efficient and practically implementable method to signal at optical frequencies (near-infrared range) is to use intensity modulation at low duty cycles with photon-counting detectors, which may be modeled as a Poisson channel; see, e.g., [1]. Low duty cycles may be efficiently implemented with pulse-position modulation (PPM). This system has been shown to be practically implementable, and represents the current state-of-the-art system for transmitting at high power efficiencies with optical carriers, capturing current designs for deep-space and near-Earth optical links; see, e.g., [2]. Hence, we model the channel as a Poisson PPM channel.

The link equation presented captures first-order parameters of the link, and abstracts out some of the low-level details involved in a more detailed, and more accurate, link budget. Doing so enables one to see the high-level trade-offs between parameters and their first-

* Google Inc.; formerly Communications Architectures and Research Section.
† Communications Architectures and Research Section.

The research described in this publication was carried out by the Jet Propulsion Laboratory, California Institute of Technology, under a contract with the National Aeronautics and Space Administration.

order impacts on link performance. This is motivated in part by cases where one wants to rapidly evaluate a number of link budgets; for example, to perform trade studies on data volumes returned by various ground terminals. In these cases, determining a highly accurate link budget for each point may be computationally prohibitive and unwarranted. Moreover, one is often interested in relative changes, which may be quickly, and even analytically, determined with the link equation.

We draw comparisons to analogous link equations for a coherently modulated and detected link with a carrier presumed to lie in the microwave regime. As a shorthand, throughout we refer to the Poisson PPM link as an *optical* link, and to the coherently modulated and detected microwave link as an *RF* link.

The article is organized as follows. In Section II, we provide the shared received power equation; in Section III, we restate the well-known RF link equation; in Section IV, we develop an optical link equation, illustrating limiting cases where certain constraints are active. In Section V, we demonstrate the accuracy of the link equation by comparison with a link budget tool, and use the equation to identify a critical data rate below which background noise begins to degrade performance.

II. Received Power

The received power for either the RF or optical signal is given by

$$P_r = \mathrm{EIRP} \cdot G \cdot L \cdot \eta \tag{1}$$

where EIRP is the effective isotropic radiated power,

$$G = \left(\frac{\pi D}{\lambda}\right)^2 \tag{2}$$

is the receive antenna gain for effective diameter D,

$$L = \left(\frac{\lambda}{4\pi R}\right)^2 \tag{3}$$

is the space loss at wavelength λ and range R, and η is the system efficiency. We would like to determine what data rate may be transmitted over the link for a given received power. This will depend on how the signal is modulated and detected, and on any noise that degrades the detection and estimation process. We refer to the equation relating the data rate, received signal and noise power, and other relevant link parameters as the *link equation*.

III. Coherent Microwave (RF) Link Equation

Let R_b denote the information data rate (bits/second) to be transmitted over the channel. The channel capacity is the maximum data rate that may be transmitted reliably. The capacity of the power- and bandwidth-constrained RF Gaussian channel is given by [3]

$$C_{\mathrm{RF}} = W\log_2\left(1+\frac{P_r}{kTW}\right) \quad (\mathrm{b/s}) \tag{4}$$

$$\approx \frac{1}{\ln(2)}\frac{P_r}{kT} \quad (\mathrm{b/s}) \tag{5}$$

where W is the bandwidth occupied by the signal, k is Boltzmann's constant in joules per kelvin, and T is the system noise temperature in kelvins. Approximation (5) follows from assuming $P_r = kTW \ll 1$, i.e., that one operates in the power-limited, as opposed to bandwidth-limited, regime. Putting $R_b \leq C_{\mathrm{RF}}$, substituting the expression for P_r in Equation (1), and rearranging terms, we have

$$\left(\frac{1}{R^2}\right)\left(\frac{G}{T}\right)\left(\frac{1}{R_b}\right) \geq \frac{\ln(2)(4\pi)^2 k}{\eta \mathrm{EIRP}\lambda^2}. \tag{6}$$

Equation (6) is a bound on the condition required to close the link. We may take Equation (6) to be the RF link equation.[1] For a given system efficiency and spacecraft transmitter terminal $(\eta, \mathrm{EIRP}, \lambda)$, the right-hand side is fixed. The left-hand side then provides the required condition to close the link with the given data rate, range, and receive antenna, which specifies (G/T). The equation facilitates interpreting the impact of changing parameters on the link. In the following section, we derive several analogous equations for the optical link.

IV. Direct-Detected Infrared (Optical) Link Equation

The capacity of the Poisson PPM channel is a function of the PPM order, and the received noise and signal rates. When only signal photoelectrons are present, we have

$$C_{\mathrm{OPT}} = \frac{\log_2 M}{MT_s}\left(1-e^{-MP_rT_s/\mathcal{E}}\right) \quad (\mathrm{b/s}) \tag{7}$$

where M is the PPM order, T_s is the slot width, and $\mathcal{E} = hc/\lambda$ is the energy per photon (h is Planck's constant and c is the speed of light). The maximum supportable $1/T_s$ is analogous to the bandwidth W in the RF case. In the optical domain, the maximum supportable $1/T_s$ is typically limited by the maximum processing speed of the transmitter and receiver, the laser pulse width, and clock accuracy.

For nonzero background power, the capacity of this channel is given by [4]

$$C_{\mathrm{OPT}} = \frac{1}{MT_s}\Big(D\big(p_1 \,\|\, p_0\big) - D\big(p_{\mathrm{y}} \,\|\, p_{\mathrm{y}|\mathbf{0}}\big)\Big) \quad (\mathrm{b/s}) \tag{8}$$

where $D(f\|g) = E_f \log_2 f/g$ is the relative entropy, p_1 and p_0 are probability mass functions of a signal and noise slot, and p_{y} and $p_{\mathrm{y}|\mathbf{0}}$ are the probability mass functions of a random PPM symbol and a noise vector, respectively. Evaluating Equation (8) requires one to approximate a multidimensional infinite sum or perform a Monte Carlo simulation. This does

[1] B. MacNeal, "Outline of MSTA's RF Downlink Calculation," JPL Interoffice Memorandum (internal document), Jet Propulsion Laboratory, Pasadena, California, 2012.

not lend itself to deriving a simple link equation. However, we may approximate Equation (8) by combining a number of bounds on C_{OPT} [5]

$$C_{\mathrm{OPT}} \approx \frac{1}{\mathcal{E}\ln(2)}\left(\frac{P_r^2}{P_r\frac{1}{\ln(M)}+P_n\frac{2}{M-1}+P_r^2\frac{MT}{\ln(M)\varepsilon}}\right)\ (b/s) \tag{9}$$

where P_n is the detected noise power.

From Equation (9), we see that as we vary P_r with P_n fixed, we sweep out three regions of operation, depending on which term in the denominator dominates. When $P_r/\ln(M) \gg 2P_n/(M-1)$ and $P_r/\ln(M) \gg P_r^2 MT_s/(\ln(M)\mathcal{E})$, the background noise is negligible, and we are in the (signal) power-constrained region. When $2P_n/(M-1) \gg P_r/\ln(M)$ and $2P_n/(M-1) \gg P_r^2 MT_s/(\ln(M)\mathcal{E})$, we are dominated by background noise. At sufficiently large P_r, the third term dominates, the capacity saturates at $\log_2(M)/MT_s$, and we are in the bandwidth-constrained region. Depending on the noise power, we may see only two of the three regimes as a function of P_r.

When the bandwidth constraint is inactive, we have

$$C_{\mathrm{OPT}} \approx \frac{1}{\mathcal{E}\ln(2)}\left(\frac{P_r^2}{P_r\frac{1}{\ln(M)}+P_n\frac{2}{M-1}}\right)\ (b/s). \tag{10}$$

This approximation is analogous to Equation (5) for the RF channel. Up to this point, we have been implicitly assuming the system efficiency η is invariant to P_r and P_n. However, this is not the case in practice. We address one deviation from this assumption in the following. Because the background noise is spatially uniform in the focal plane and the signal power is not, it follows that one can improve the system performance with a spatial filter, collecting power only over a finite region of the focal plane.[2] This may be done with an iris, or via signal processing on the outputs of a detector array. The optimum setting of the spatial filter depends on the incident signal and noise power, as well as the spatial distribution of the signal power. Having this attenuation depend on the signal and noise power would nominally complicate the definition of a link equation. We address this in the next section.

A. Setting the Field of View: Spatial Filtering of Signal and Noise

We factor the system efficiency as $\eta = \eta'\eta_{\mathrm{FOV}}$, where η_{FOV} denotes the fraction of the signal collected by a spatial filter. In this section, we'll show that, to a reasonable approximation, we may take η_{FOV} to be a constant.

Let $I(x,y)$ be the normalized mean signal intensity function in the focal plane, such that

$$\int_{(x,y)\in\mathcal{A}} I(x,y)\,dxdy \tag{11}$$

[2] In the RF case, incident background noise is assumed to be negligible relative to thermal noise in the simplified link equation. For the optical channel, incident background noise is the dominant noise source.

is the fraction of the received signal power collected in area $\mathcal{A}$. We model $I(x,y)$ as Gaussian[3]

$$I(x,y) = \frac{1}{2\pi\sigma^2}\exp\left(\frac{-(x^2+y^2)}{2\sigma^2}\right) \tag{12}$$

with

$$\sigma = \left(0.42\lambda F\right)\sqrt{\left(\frac{1}{r_0}\right)^2 + \left(\frac{1}{D}\right)^2} \tag{13}$$

where F is the telescope focal length and r_0 is the atmospheric coherence length along the line of sight. Let δ be the radius of the collecting area in the focal plane, which we presume is populated with a collection of photon-counting photodetectors, and define a field of view (FOV) parameter

$$\gamma \stackrel{\text{def}}{=} \frac{\delta^2}{2\sigma^2}, \tag{14}$$

which is the ratio of the collecting area to the area of the signal intensity function at $I(x,y) = I(0,0)/e$. Then we have

$$\eta_{\text{FOV}} = 1 - e^{-\gamma}. \tag{15}$$

One would like to choose δ, or, equivalently, γ, to maximize the channel capacity. To determine this value, we must first determine the impact of γ on the noise power.

We assume the noise is dominated by sky radiance, such that [6]

$$P_n = \frac{(\Delta_\lambda I_b \Omega)\pi D^2}{4} \tag{16}$$

where Δ_λ is the bandwidth of a narrowband spectral filter that rejects noise outside a bandwidth around the carrier, Ω is the detector field-of-view, and I_b is the background sky radiance (W/m^2 sr μm) incident on the aperture. For small angles, we have $\Omega \approx \pi(\delta/F)^2$, and, substituting γ, we have

$$\Omega \approx (0.35)\pi\gamma\lambda^2\left(\frac{1}{r_0^2} + \frac{1}{D^2}\right) \approx 0.35\pi\gamma\frac{\lambda^2}{r_0^2} \tag{17}$$

where the second approximation holds for $D \gg r_0$.

We see from Equation (16) and Equation (17) that the noise power grows linearly in γ, while, from Equation (15), that the signal power saturates, growing as $(1 - e^{-\gamma})$. Hence, there is a capacity-maximizing γ: a function of the incident signal intensity, noise radiance, and spatial distribution of the signal, characterized by σ.

[3] S. Piazzolla, personal communication, Jet Propulsion Laboratory, Pasadena, California, n.d.

In [7]. it is shown that, to a good approximation, the increase in signal power required to close the link with $\gamma = 2.44$ is less than 0.4 dB relative to the optimum choice. To simplify the development of a link equation, in the remainder we put $\gamma = 2.44$ in all cases.[4] Then the detected signal power is given by Equation (1) and Equation (15) and the detected noise power by

$$P_n = \frac{I_n \pi D^2}{4} \tag{18}$$

where

$$I_n = \Delta_\lambda I_b \Omega = \Delta_\lambda I_b (0.35) \pi \gamma \lambda^2 \left(\frac{1}{r_0^2} + \frac{1}{D^2} \right) \tag{19}$$

is the noise irradiance in the aperture plane, with units of W/m^2. Note that if $D \gg r_0$, then I_n depends only on the receive telescope via Δ_λ.

B. Link Equation for Fixed *M*, Power-Constrained Regime

First consider, analogous to the RF case, the power-constrained regime (inactive bandwidth constraint). Substituting P_r in Equation (1) and P_n in Equation (18) into Equation (10), we have

$$\begin{aligned} C_{\mathrm{OPT}} &\approx \frac{1}{\mathcal{E} \ln(2)} \left(\frac{EIRP \cdot G \cdot \dfrac{\lambda^2}{(4\pi)^2} \dfrac{1}{R^2} \cdot (1 - e^{-\gamma})}{\dfrac{1}{\ln(M)} + \dfrac{P_n}{P_r (1 - e^{-\gamma})} \dfrac{2}{M-1}} \right) \\ &= EIRP \cdot \frac{G}{(1+K)} \cdot \frac{1}{R^2} \cdot \frac{\ln(M)}{\ln(2)\mathcal{E}} \cdot \left(1 - e^{-\gamma}\right) \cdot \frac{\lambda^2}{(4\pi)^2} \quad \text{(b/s)} \end{aligned} \tag{20}$$

where

$$K = \frac{2 \ln(M)}{(M-1)(1 - e^{-\gamma})} \frac{P_n}{P_r}. \tag{21}$$

Note that K is a function of the range R and gain G. Putting $R_b \leq C_{\mathrm{OPT}}$, and rearranging terms yields an optical link equation for this regime:

$$\left(\frac{1}{R^2} \right) \left(\frac{G}{1+K} \right) \left(\frac{1}{R_b} \right) \gtrsim \frac{\ln(2)(4\pi)^2 \mathcal{E}}{\ln(M) \mathrm{EIRP} (1 - e^{-\gamma}) \lambda^2}. \tag{22}$$

The link equation divides into two regions: a shot-noise, or signal-dominant, region for large P_r / P_n, and a noise-limited region for small P_r / P_n:

$$\left(\frac{1}{R^2} \right) G \left(\frac{1}{R_b} \right) \gtrsim \frac{\ln(2)(4\pi)^2 \mathcal{E}}{\ln(M)(1 - e^{-\gamma}) \mathrm{EIRP} \lambda^2}, \quad K \ll 1 \tag{23}$$

[4] Note that this presumes the detector area can be sufficiently large to encircle a certain fraction of the signal in all cases.

$$\left(\frac{1}{R^4}\right)\left(\frac{G}{I_n}\right)\left(\frac{1}{R_b}\right) \gtrsim \frac{\ln(2)(4\pi)^4\mathcal{E}}{\pi(M-1)\left((1-e^{-\gamma})\mathrm{EIRP}\right)^2\lambda^2}, \quad K \gg 1 \tag{24}$$

The link behaves differently in these two regions. For large K, the rate is proportional to $1/R^4$, and the link is degraded by background light such that the receive telescope has a contribution G/I_n analogous to G/T for the RF regime. For small K, the rate is proportional to $1/R^2$, and the performance is not affected by background light. These two regions of operations are consistent with the results found in an earlier study [5].

C. Link Equation for Varying *M*, Bandwidth-Constrained Regime

In many cases, the PPM order may be varied over the mission. This is done only when the bandwidth constraint is active, since, with no bandwidth constraint, the capacity is strictly increasing in the PPM order, and one would always use the largest available M. When one is bandwidth limited, the PPM order may be decreased in order to signal at a higher data rate. In order to reflect this, we introduce a bandwidth constraint, which we state as a minimum supportable slot width T_{min}. Substituting P_r in Equation (1) and P_n in Equation (18) into Equation (9), we have

$$\begin{aligned} C_{\mathrm{OPT}} &\approx \frac{\ln(M)}{\mathcal{E}\ln(2)}\left(\frac{EIRP\cdot G\cdot\frac{\lambda^2}{(4\pi)^2}\frac{1}{R^2}\cdot(1-e^{-\gamma})}{1+K+EIRP\cdot G\cdot L\cdot(1-e^{-\gamma})\frac{MT_s}{\mathcal{E}}}\right) \\ &= EIRP\cdot\frac{G}{(1+K+\frac{I_sMT_sG\lambda^2(1-e^{-\gamma})}{\mathcal{E}4\pi})}\cdot\frac{1}{R^2}\cdot\frac{\ln(M)}{\ln(2)\mathcal{E}}\cdot(1-e^{-\gamma})\cdot\frac{\lambda^2}{(4\pi)^2} \quad \text{(b/s)} \end{aligned} \tag{25}$$

where $I_s = \frac{EIRP\cdot 4\pi\cdot L}{\lambda^2}$ is the signal irradiance in W/m². Putting $R_b \le C_{\mathrm{OPT}}$, and rearranging Equation (25) gives us a link equation with bandwidth constraint:

$$\left(\frac{1}{R^2}\right)\left(\frac{G}{1+K+\frac{I_sMT_sG\lambda^2(1-e^{-\gamma})}{\mathcal{E}4\pi}}\right)\left(\frac{1}{R_b}\right) \ge \frac{(4\pi)^2\mathcal{E}}{\mathrm{EIRP}\log_2(M)\lambda^2(1-e^{-\gamma})}. \tag{26}$$

For a given T_s, Equation (9) has a capacity-maximizing M. This may be found by evaluating Equation (9) (which we conjecture is convex in M) numerically. Suppose $P_r \gg P_n$, such that

$$C_{\mathrm{OPT}} \approx \frac{\ln(M)}{\ln(2)\mathcal{E}}\left(\frac{P_r}{1+P_r\frac{MT_s}{\mathcal{E}}}\right). \tag{27}$$

Allowing M to be real-valued, differentiating Equation (27) with respect to M and solving yields

$$\log_2(M^*) \approx \frac{\left(1+W\left(\frac{\mathcal{E}}{eP_rT_s}\right)\right)}{\ln(2)} \tag{28}$$

where $W(\cdot)$ is the Lambert-W function. Equation (28) approximates the optimum M in the power- and bandwidth-constrained region. Figure 1 illustrates M^* given by Equation (28) compared to the optimum M found by numerical evaluation of the power- and bandwidth-constrained capacity, Equation (7), as a function of the mean signal photon number $N_s = P_r T_s / \mathcal{E}$. As one moves into the noise-limited regime, Equation (28) may be used as a lower bound on the optimum M.

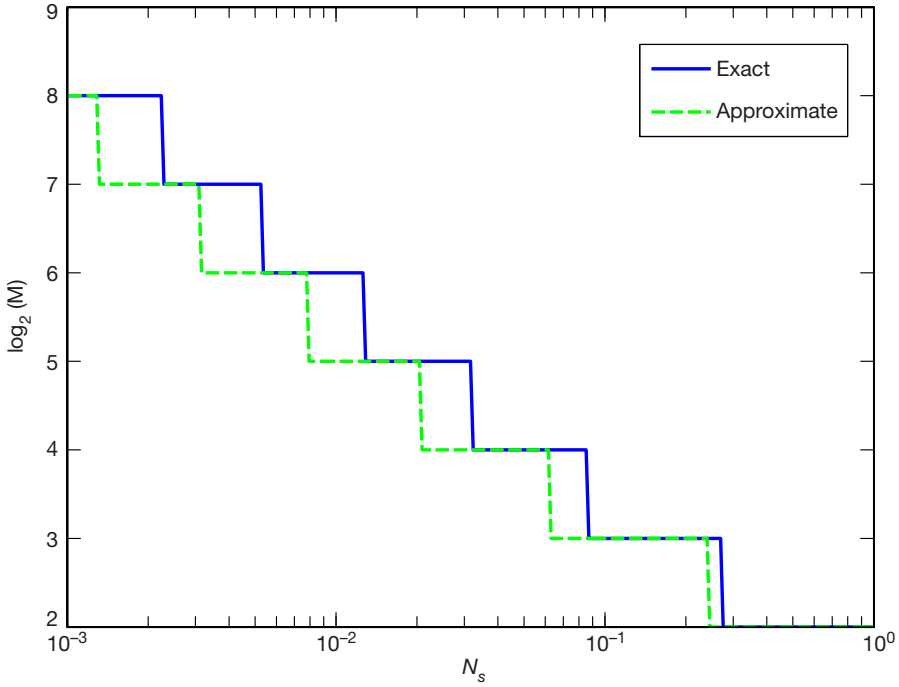

Figure 1. Optimum *M* for noiseless ($P_n = 0$) channel as a function of the mean signal photon number $N_s = P_r T_s / \mathcal{E}$. Exact from numerical evaluation of capacity, noiseless prediction from Equation (28).

D. Antenna *G/T*

In the RF link equation, the dominant noise term is assumed to be the noise temperature of the receiver, and in Equation (6), we see that the fraction (G/T) is sufficient to characterize the impact of a particular receive antenna on an RF link — any antenna with the same (G/T) will provide the same performance. The analogous term for an optical antenna, from Equation (22) is

$$\left(\frac{G}{1 + \frac{2\ln(M)}{M-1}\frac{I_n}{I_s}} \right)$$

which is a function of the ratio I_s/I_n. With the optical link, the dominant noise term is due to sky radiance, which is not a property of the antenna (except insofar as the antenna location is a contributing factor). Hence, we cannot capture the antenna gain and noise in a single term analogous to G/T. In the two asymptotic regions, the term reduces to a constant multiple G or G/I_n. In general, the pair (G/I_n) is required to characterize an optical telescope, and there is no single parameter analog to G/T that captures the impact of the antenna and noise under all conditions.

V. Applications and Accuracy

In this section, we examine the accuracy of the simplified link equation, and illustrate an example of its application, determining a critical data rate below which background noise begins to degrade the performance.

A. Accuracy

The accuracy of the simplified link equation is determined by comparing supportable data rates predicted with the link equation to that predicted by the Strategic Optical Link Tool (SOLT). The SOLT is built off the Deep Space Optical Link (DeSol) software,[5] which was designed to generate link budgets with sufficient accuracy for mission design. SOLT is a modification of DeSOL designed to operate as part of the Space Communications Mission Model (SCMM) tool suite. In its nominal form, SOLT utilizes its own bound on the channel capacity, trading off run-time for accuracy. We also developed a variation of the software called Fast-SOLT that incorporated the optical link equation and analytic field of view. In this article, however, we use the term SOLT to refer to its nominal form.

Nominal SOLT differs from our simplified link equation in a number of ways. While a full description of SOLT is beyond the scope of this article, we point out a few significant differences in the computation of a supportable data rate. SOLT performs an optimization over the field of view, including contributions from detector dark noise. It takes into account several signal-dependent loss factors, such as a finite extinction ratio, and losses due to detector jitter, which are a function of the slot width. It also allows non-extended noise sources, while the link equation assumes only an extended noise source. We may take SOLT to be representative of a high-resolution link equation for the purpose of our comparison. In order to measure the accuracy of the simplified link equation, it is compared to the results from SOLT generated by numerically evaluating Equation (8), which we take to be the true value.

The link equations presented in Section IV allow any real-valued data rate. In practice, data rates are restricted to a finite number of choices given by the allowable signaling parameters. The data rate of a PPM modulation signal with error-control code (ECC) rate R_{ECC}, PPM order M, and slot width T_s is given by

$$R_b = R_{ECC} \frac{\log_2 M}{M T_s} \quad \text{(b/s)}. \tag{29}$$

Practical systems have a minimum supportable slot width T_{min} due to hardware limitations. A finite set of slot widths is typically supported. Our implementation of SOLT constrains slot width to be 1 dB steps relative to T_{min}: $\{T_{min}, 1.26\,T_{min}, 1.58\,T_{min}, \ldots\}$. Practical systems also allow only a finite set of supportable ECC rates. In all our examples, we put $R_{ECC} = 1/2$, a choice that represents a number of proposed designs. In order to reflect these constraints in the link equation (9), we choose the largest $R_b = R_{ECC} \frac{\log_2 M}{M T_s}$ such that $C_{\text{OPT}} > R_b$ with

[5] S. Piazzolla, Deep Space Optical Link (DeSOL) software, Optical Communications Group, Jet Propulsion Laboratory, Pasadena, California, 2008.

C_{OPT} given by Equation (9) — note that Equation (9) depends on (M, T_s). Since the collection of allowable (M, T_s, R_{ECC}) is typically small, an optimization over (M, T_s, R_{ECC}) is simple to implement.

Figure 2 illustrates achievable data rates for a 2017–2019 Mars to Mount Graham trajectory with link parameters based on the Deep-space Optical Terminals (DOT) concept study [8]. In Figure 2, we adopted a clear-sky atmospheric model, a code rate of $R_{ECC} = 0.5$, $T_{min} = 0.5$ ns, and a fixed modulation order $M = 16$. Illustrated are the achievable data rates computed from SOLT and from link equation (9), both quantized to allowable data rates, as described above. We see good agreement between SOLT predictions and Equation (9). We also illustrate data rates predicted by Equation (9) with no restriction on R_{ECC}. In this case, the tool always chooses $T_s = T_{min}$, and scales R_{ECC} to close the link. This is a simple upper bound to the data rate for fixed R_{ECC} and requires no optimization over (M, T_s, R_{ECC}).

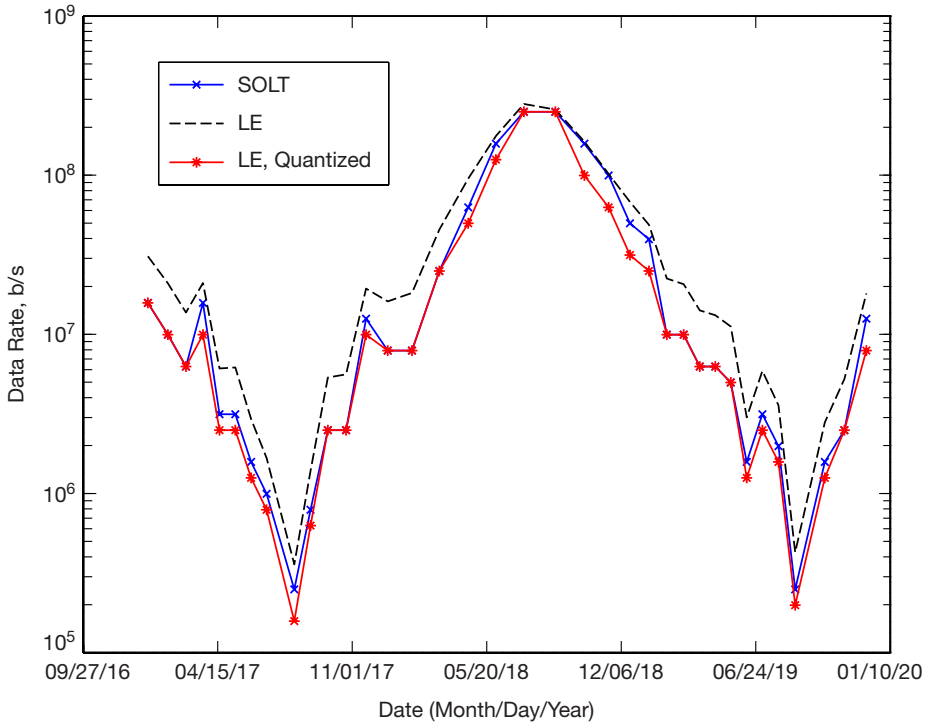

Figure 2. Achievable data rates for a Mars–Earth link, T_{min} = 0.5 ns, M = 16. Predictions from SOLT, Equation (9) constrained to the rates allowed by SOLT, and Equation (9) with any R_{ECC}.

Figure 3 illustrates achievable data rates for the same trajectory but allowing $M \in \{16, 32, 64, 128\}$. Proposed missions vary the PPM order to more efficiently map received signal power to a data rate. As in the prior figure, the prediction from SOLT and the link equation is illustrated, showing good agreement. The rates achieved by allowing any R_{ECC}, but optimizing over M, are also shown. Figure 4 illustrates the ratios

$$R_{b,LE}/R_{b,SOLT}$$

where $R_{b,LE}$ is the prediction from the link equation, and $R_{b,SOLT}$ from SOLT. We see that in most cases, data rate is within 75 percent of the more accurate estimate from SOLT. In many

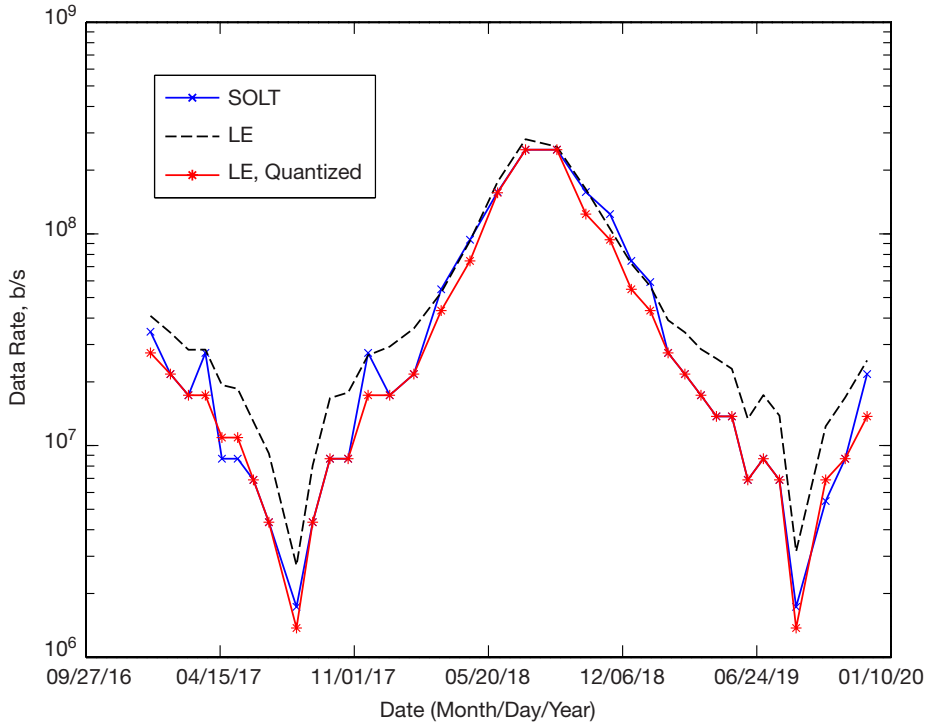

Figure 3. Achievable data rates for a Mars–Earth link, T_{min} = 0.5 ns, $M \in \{16,32,64,128$. Predictions from SOLT, Equation (9) constrained to the rates allowed by SOLT, and Equation (9) with any R_{ECC}.

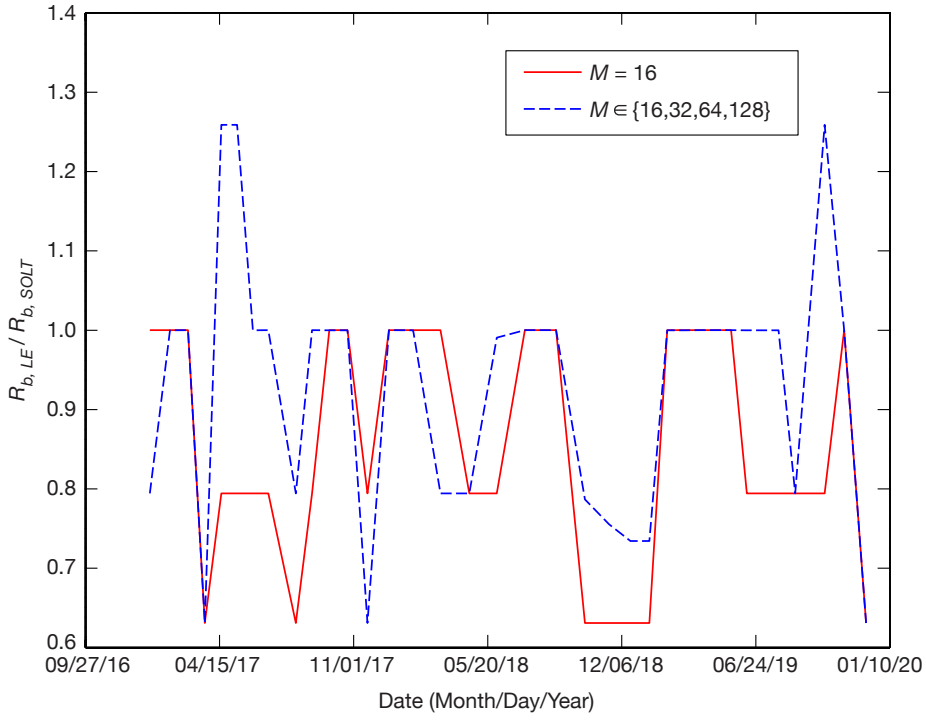

Figure 4. The ratios $R_{b,LE}/R_{b,SOLT}$ from Figures 2 and 3, illustrating a fractional error in the link equation of less than 40 percent in all cases.

cases, this is sufficiently accurate. In particular, for aspects of design where one needs not the absolute data rate but to know relative data rates, say, for optimization, we conjecture that the link equation preserves the ordering that would be given by a more accurate measure.

B. Application: Critical Data Rate

We would like to know under what conditions we fall into one of the two regimes identified by Equation (23) and Equation (24). One can view the driving parameter as the target data rate as follows. Setting $R_b \leq C_{OPT}$ and substituting C_{OPT} in Equation (7), we compute the minimum receive signal power required to support data rate R_b in Equation (29):

$$R_{ECC}\frac{\log_2 M}{MT_s} \leq \frac{\log_2 M}{MT_s}\left(1 - e^{-MP_r T_s/\mathcal{E}}\right).$$

Assuming $R_{ECC} = 0.5$ and rearranging terms, we have

$$P_r \geq \frac{\ln(2)\mathcal{E}}{MT_s}.$$

Now if the noise level is such that $K \ll 1$, then background noise will be negligible. Rearranging terms and substituting the minimum received power required to support the given data rate, the condition on the noise power such that we are in the $(1/R^2)$ regime is

$$P_n \ll R_b\left(\frac{(M-1)\mathcal{E}(1-e^{-\gamma})}{(\log_2 M)^2}\right). \tag{30}$$

The noise power is independent of the spacecraft (EIRP and range R). Hence, Equation (30) gives a condition on a critical noise power as a function of the target data rate and PPM order at which the link will transition from a signal-dominant to noise-dominant regime. This is the manner in which we typically approach a link design. Suppose we are designing an Earth–Mars link. The ground telescope is usually fixed (or drawn from a small set) and the link geometry (establishing range, sky radiance, and seeing) is also fixed. This fixes P_n. The designer adjusts the spacecraft resources (EIRP, P_t) to support a desired R_b. Equation (30) establishes a critical data rate above which the link will operate in the signal-dominant regime. For example, for the link illustrated in Figure 5, the noise power is below 10^{-12} W up to about 2.0 AU. Inverting this gives a critical data rate on the order of 10 Mbps. Figure 5 illustrates the data from Figure 2 plotted as R_b versus R. We see a transition from $(1/R^2)$ to $(1/R^4)$ behavior around 10 Mbps. The rate drops off faster than $1/R^4$ beyond this range because the range is increasing *and* P_n is increasing. The rate of change of the noise power below the signal rate required for 10 Mbps is irrelevant, so long as it remains below 10^{-12} W.

VI. Conclusions

We have developed a link equation for the direct-detected Poisson PPM channel. We demonstrated the accuracy of the equation by comparing its predictions to those provided by a

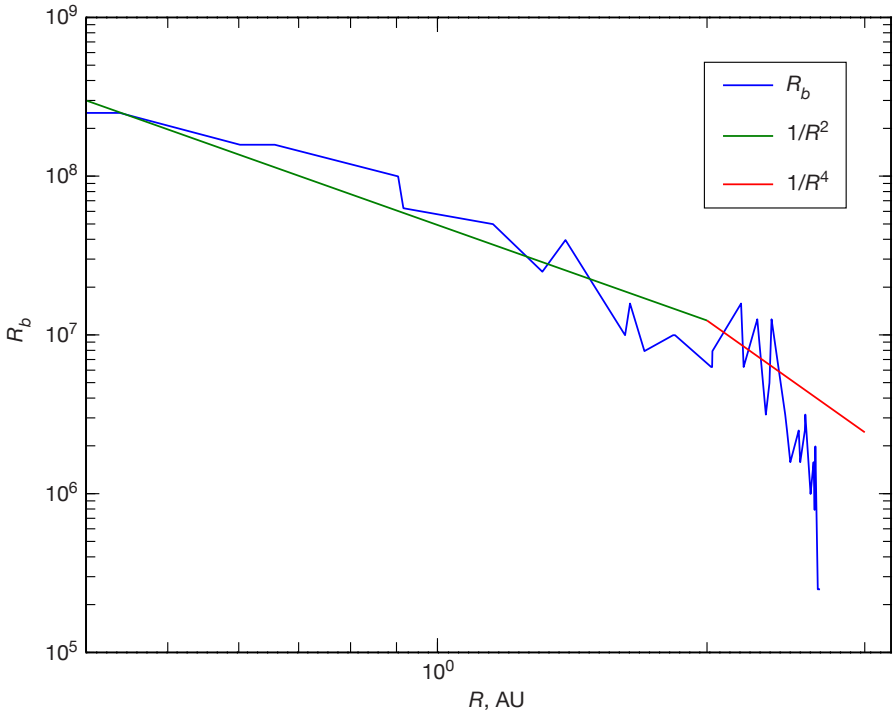

Figure 5. Data rate as a function of range (in AU) for the sample Earth–Mars link from Figure 2, illustrating a critical data rate at ~10 Mbps.

link budget tool with exact computation of the channel capacity. The agreement is sufficiently good to justify using the equation for approximate analysis of an optical link. We find this useful in understanding the relationships between contributing parameters on an optical link. We demonstrated one such use, deriving a critical data rate at which the link transitions from being signal dominant to background noise dominant.

References

[1] B. Moision and J. Hamkins, "Deep-Space Optical Communications Downlink Budget: Modulation and Coding," *The Interplanetary Network Progress Report*, vol. 42-154, Jet Propulsion Laboratory, Pasadena, California, pp. 1–28, April–June 2003, article dated August 15, 2003.
http://ipnpr.jpl.nasa.gov/progress_report/42-154/154K.pdf

[2] B. S. Robinson, D. M. Boroson, D. A. Burianek, and D. V. Murphy, "Overview of the Lunar Laser Communications Demonstration," *Proceedings of SPIE*, vol. 7923, 2011.

[3] T. M. Cover and J. A. Thomas, *Elements of Information Theory*, New York: John Wiley & Sons, 1991.

[4] J. Hamkins, M. Klimesh, R. McEliece, and B. Moision, "Capacity of the Generalized PPM Channel," *Proceedings of the International Symposium on Information Theory*, ISIT 2004, June 20–July 2, 2004, page 334, 2004.

[5] B. Moision and W. Farr, "Range Dependence of the Optical Communications Channel," *The Interplanetary Network Progress Report*, vol. 42-199, Jet Propulsion Laboratory, Pasadena, California, pp. 1–10, November 15, 2014.
http://ipnpr.jpl.nasa.gov/progress_report/42-199/199B.pdf

[6] A. Biswas and S. Piazzolla, "Deep-Space Optical Communications Downlink Budget from Mars: System Parameters," *The Interplanetary Network Progress Report*, vol. 42-154, Jet Propulsion Laboratory, Pasadena, California, pp. 1–38, April–June 2003, article dated August 15, 2003.
http://ipnpr.jpl.nasa.gov/progress_report/42-154/154L.pdf

[7] B. Moision, "The Capacity-Maximizing Field of View of an Optical Communications System," *The Interplanetary Network Progress Report*, vol. 42-190, Jet Propulsion Laboratory, Pasadena, California, pp. 1–12, August 15, 2012.
http://ipnpr.jpl.nasa.gov/progress_report/42-190/190A.pdf

[8] A. Biswas, H. Hemmati, S. Piazzolla, B. Moision, K. Birnbaum, and K. Quirk, "Deep-space Optical Terminals (DOT) Systems Engineering," *The Interplanetary Network Progress Report*, vol. 42-183, Jet Propulsion Laboratory, Pasadena, California, pp. 1–38, November 15, 2010.
http://ipnpr.jpl.nasa.gov/progress_report/42-183/183A.pdf